NATIONAL AERONAUTICS AND SPACE ADMINISTRATION

Technical Report 32-1377

Large-Amplitude Resonant Combustion in Liquid Rocket Engine Chambers: Some Aspects of Initiation

A. A. Kovitz

JET PROPULSION LABORATORY
CALIFORNIA INSTITUTE OF TECHNOLOGY
PASADENA, CALIFORNIA

November 15, 1969

NATIONAL AERONAUTICS AND SPACE ADMINISTRATION

Technical Report 32-1377

Large-Amplitude Resonant Combustion in Liquid Rocket Engine Chambers: Some Aspects of Initiation

A. A. Kovitz

JET PROPULSION LABORATORY
CALIFORNIA INSTITUTE OF TECHNOLOGY
PASADENA, CALIFORNIA

November 15, 1969

Prepared Under Contract No. NAS 7-100
National Aeronautics and Space Administration

Preface

The work described in this report was performed by the Propulsion Division of the Jet Propulsion Laboratory. The author is a member of the Department of Mechanical Engineering and Astronautical Sciences, Northwestern University, Evanston, Ill. This work was performed during the author's stay at the Laboratory in the summer of 1968.

Acknowledgment

The author is happy to thank Jack H. Rupe for suggesting this study and for his interest in its progress. Dr. Raymond O. Kushida was particularly helpful during many discussions. His insights were most illuminating. Discussions with Richard M. Clayton concerning his experimental results and knowledge of resonant burning were indispensable.

Contents

I. Introduction 1

II. The Classical Blast Wave 2

III. Application of the Zel'dovich, Kogarko, Simonov Model for Initiation of Spherical Detonation Waves 3

IV. The Interaction of Reactive Wave Fronts With Walls and Gaseous Interfaces 6

A. Phenomenological Description and Analytical Formulation 6

B. Reflection of Chapman–Jouguet Detonation as a Shock Wave 8

C. Reflection of Chapman–Jouguet Detonation in the Presence of a Gaseous Interface 9

V. The Transition of Spherical Detonation to a Rotating Combustion Disturbance 11

VI. Conclusions 12

Nomenclature 12

References 13

Appendix. Rocket Motor and Thermochemical Data 15

Table

1. Zel'dovich, Kogarko, Simonov model for spherical detonation 5

Figures

1. Normal reflection of a wave front from a wall 3
2. Spherical detonation wave 4
3. Spherical detonation wave according to Eq. (6) 4
4. Motion of wave front 8
5. Transmission and reflection of wave front at gaseous interface; reflection of transmitted wave from wall 9
6. Overall reflected pressure ratio as function of temperature ratio at gaseous interface 10
7. Transition of a spherical detonation to a rotating combustion disturbance 11

Abstract

The initiation of large-amplitude, high-frequency resonant combustion in rocket chambers is considered as the result of a finite disturbance. It is shown that a relatively low-energy blast wave can initiate a spherical detonation wave, which may act as the source of such instability. The wave's interaction with a hot–cool gaseous interface and subsequent reflection from the chamber wall can produce the high amplitudes observed. A descriptive explanation of the transition from spherical detonation to a rotating combustion-driven wave is presented. The analysis suggests that high temperatures, nearly complete combustion, and non-symmetrical conditions within the chamber are likely to lead to the "sudden" initiation of resonant burning.

Large-Amplitude Resonant Combustion in Liquid Rocket Engine Chambers: Some Aspects of Initiation

I. Introduction

It is well known that the combustion processes in rocket engines do not always proceed in a steady fashion. Time- and space-wise variations in chamber pressure (both large and small amplitudes at high and low frequencies) are relatively direct indicators of the occurrence of nonsteady combustion. Since time and space variations of the rate of burning may be accompanied by deleterious effects on engine performance and/or endanger the engine's structural integrity, the understanding and control of unstable combustion is an important aspect of rocket engine design.

This report will focus attention on a particular type of combustion instability that seems to be common in flight engines and is reproducible in test engines. In its fully developed state, it is characterized by high frequency ($\gtrsim$1000 Hz) and large relative amplitude ($\sim$two to ten times the intended chamber operating pressure); see Ref. 1. Furthermore, its initiation seems to be almost instantaneous; i.e., there is no detectable period of amplification of presumably initially low-amplitude pressure disturbances.

Clayton, Rogero, and Sotter (Ref. 2) have made extensive observations of such steep-fronted, high-amplitude pressure waves in liquid-propellant rocket chambers. Using multiple high-response pressure transducers, they find that the instability appears suddenly and takes on its long-time character within a time corresponding to as little as one or two periods of the fully developed oscillatory mode. The fully developed mode (resonant burning) is shown to consist of a rotating detonation-like wave moving peripherally around the rocket chamber; its pressure amplitude and frequency correspond to those found in flight engines using the same type of propellants and having the same order of thrust.

These experimental results are difficult to interpret in terms of a linearized theory (Ref. 3) of combustion instability. The large-amplitude, steep-fronted wave that immediately precedes the resonant burning mode cannot easily be explained as the result of the growth of a small disturbance amplified by classical resonance phenomena; it is more natural to conceive of it as being initiated by a finite disturbance within the chamber. This is the point

of view taken in this report. A phenomenological description of the transition to detonation of an arbitrary local energy source in a reactive medium will be developed. Order-of-magnitude calculations to support the concept will be presented and applied to test data. The subsequent interaction of the generated wave with the wall and with a gaseous interface will also be estimated.

Finally, a descriptive argument will be given for the transition of the spherical detonation-like wave to the observed rotating disturbance as found in Clayton's experiments (Ref. 2).

II. The Classical Blast Wave

Bonnell (Ref. 4) has performed computations and experiments on the effect of exploding a bomb within the rocket chamber; experiments were conducted both in an operating (hot) rocket chamber and in an inert, nitrogen-pressurized (cold) rocket chamber. The results indicated that one does observe pressure waves similar to those found during resonant burning; however, the comparison between cold and hot chamber data was inconclusive.

In this section, some of his computations will be repeated, the purpose being to show that a classical blast wave (no coupling between chemical heat release and wave front after the initial explosion) alone cannot generally account for the first pressure peak observed at the wall. This conclusion will be based upon the computed ratio of required blast energy to total available chemical energy in the chamber for a given pressure amplitude. It will be seen that for high-amplitude waves this ratio is too large to be reasonable when it is also required that $E_{\text{blast}} << E_{\text{chamber}}$. Bonnell did not make such a comparison since he was using a bomb to initiate the blast wave; in his case, E_{blast} could, in principle, be any value.

All computations will be based upon the data tabulated in the Appendix. These data are typical for a large space propulsion engine using earth-storable propellants. The mass fraction of total flow rate vaporized will be taken as 50% up to 8 in. from the injector, and as *all* vaporized from that point on. This is a rough simplification of a more accurate computation based on a steady combustion computer model for an 18-in.-diam motor burning N_2O_4 + 50/50 propellants.

Landau and Lifshitz (Ref. 5) derive the similarity solution (first done by Taylor and Sedov) for a spherical blast wave. Their results may be put in the form

$$E_{\text{blast}} = \frac{25}{8}\frac{(\gamma+1)}{\xi_0^5} r_0^3 p_2 \tag{1}$$

$$t(r_0) = \left[\frac{8}{25}\frac{\rho_1/p_2}{(\gamma+1)}\right]^{1/2} r_0 \tag{2}$$

where r_0 is the distance from the center to the spherical wave front, p_2 is the pressure just behind the front, ρ_1 is the density just ahead of the front, E_{blast} is the blast energy, and $t(r_0)$ is the time measured from the instant of blast. The term ξ_0 is a mathematical constant:

$$\xi_0^5 = 1.167 \qquad \text{for } \gamma = 1.4$$

$$\xi_0^5 = 0.580 \qquad \text{for } \gamma = 1.2$$

The available chemical energy per unit mass in the chamber is nonzero only in the region where liquid spray still exists (on the assumption that vaporization is the rate-controlling factor in steady combustion). Where 50% of the mass flux is liquid, the available chemical energy per unit mass of gas–liquid mixture is

$$\frac{1}{2} \times 1200\ \text{cal/g} = 2.52 \times 10^6\ \text{m}^2/\text{s}^2$$

The density of gas in the chamber is

$$\rho_1 = p_1/RT_1 = 4.36 \times 10^{-1}\ \text{kg/m}^3$$

for

$$p_1 = 80\ \text{psia} = 5.5 \times 10^5\ \text{kg/m s}^2$$

$$T_1 = 3100°\text{K}$$

$$R = R_0/20.4 = 4.06 \times 10^6\ \text{cm}^2/°\text{K s}^2$$

The total mass of gas in the first 8 in. of the chamber (where liquid spray exists) is

$$M_g = \frac{\pi}{4} \times (18\ \text{in.})^2 \times 8\ \text{in.} \times \rho_1$$

But this is equal to the mass of liquid M_l in that region; therefore

$$E_{\text{chamber}} = 600\, M_l = 0.743 \times 10^5\ \text{kg m}^2/\text{s}^2$$

Assume that the blast wave originates on the axis of the chamber and travels to the wall, where a reflection

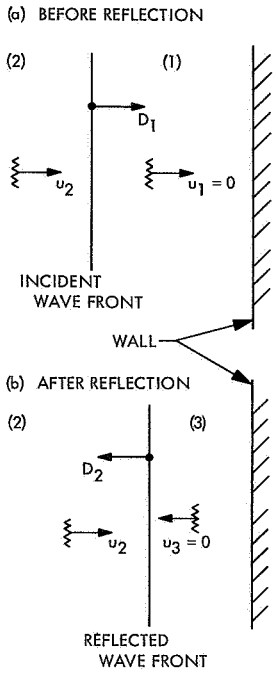

Fig. 1. Normal reflection of a wave front from a wall; u_1, u_2, u_3 are particle velocities, and D_1, D_2 are wave front velocities

must occur; the maximum increase in pressure is due to normal incidence. The maximum pressure indicated by the transducer would be p_3 (see Fig. 1). If the incident shock is "strong," then the maximum value of p_3/p_2 is $p_3/p_2 \cong 13$ for $\gamma = 1.2$ (see Ref. 6). Therefore, the minimum value of p_2 is $p_3/13$.

Experimentally, it has been shown[1] that the first observed pressure pulse is such that $p_3 \cong 700$ psia $= 4.8 \times 10^6$ kg/m s^2. With $r_0 = 9$ in. $\cong 23$ cm and $p_2 = p_3/13$, Eq. (1) yields

$$E_{\text{blast}} = 0.525 \times 10^5 \text{ kg m}^2/\text{s}^2$$

But this shows that $E_{\text{blast}}/E_{\text{chamber}} \cong 0.71$.

This means that the energy in the blast wave must be of the same order as the total available chemical energy in the chamber; of course, if the blast wave originated nearer the wall, the blast energy would decrease as r_0^3 for the same p_2 (see Eq. 1). However, experiment shows that the initial pulses are repeatable in form and amplitude and it is not reasonable to expect the pressure transducer to be in such a position as to always pick up the disturbances from an explosion very close to the wall in which the transducer is located. This computation shows that a blast wave, of itself, is probably not the observed initial pressure pulse.

For future discussion, the time for a blast wave to reach the wall, using Eq. (2), is $t(r_0 = 23\text{ cm}) \cong 9.5 \times 10^{-5}$ s.

III. Application of the Zel'dovich, Kogarko, Simonov Model for Initiation of Spherical Detonation Waves

Zel'dovich, Kogarko, and Simonov (Ref. 7) introduced a simple model for obtaining a qualitative criterion for the initiation of spherical detonation waves by blast waves. They also performed experiments that gave support to the model.

Their model is constructed as follows:

(1) At the initial instant, a quantity of energy E_{blast} is liberated in a reactive medium.

(2) During the interval $0 < t < \tau$ (where τ is a chemical induction time), the medium is disturbed in the manner of a blast wave; chemical reaction is negligible; the pressure behind the front decays as in Eq. (1).

(3) For $t > \tau$, chemical reaction begins to add thermal energy to the gas behind the propagating front; the pressure may continue to decrease until the effect of chemical reaction reverses this trend and stabilizes the pressure behind the spherical front at the steady Chapman–Jouguet pressure given by the Rankine–Hugoniot equations.

(4) Step 3 may, however, never go to completion if the pressure minimum (which always exists) is so low as to cause the chemical heat release rate to be too small; then the pressure continues to fall and the spherical wave becomes, at most, a deflagration rather than a detonation.

This description will now be given some quantitative aspects. Assume that the spherical pressure front reaches the position ΔR at $t = \tau$. From Eqs. (1) and (2),

$$\Delta R = U_1 E_{\text{blast}}^{1/5}, \qquad U_1 \equiv \xi_0 \rho_1^{-1/5} \tau^{2/5} \tag{3}$$

In this sense, ΔR is a measure of the detonation wave "thickness," at least during the early portion of its development (the true detonation wave thickness is taken to be the distance behind the pressure front that a fluid particle travels with respect to the front before chemical reaction is essentially complete). It will be seen that this estimate of the detonation wave thickness is greater than,

[1]Clayton, R. M., Jet Propulsion Laboratory, Pasadena, Calif., private communication.

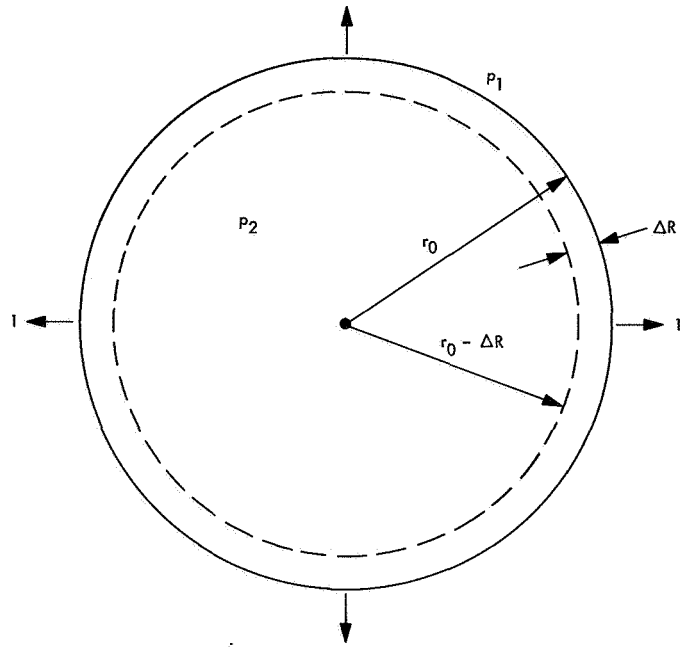

Fig. 2. Spherical detonation wave; r_0 is the position of the wave front, and ΔR is the "thickness" of the reaction zone as computed from Eq. (3)

say, $D^{C\text{-}J}\tau$ where $D^{C\text{-}J}$ is the steady Chapman–Jouguet velocity;[2] therefore, using $U_1 E_{\text{blast}}^{1/5}$ is equivalent to taking a longer chemical induction time and should yield larger required values for E_{blast}. We are being on the "safe side" since we want to compare E_{blast} with E_{chamber} and to determine whether $E_{\text{blast}} << E_{\text{chamber}}$.

For any $t > \tau$, the pressure front is at r_0 (see Fig. 2). The chemical energy liberated behind the front is given by $(4/3)\,\pi\,(r_0 - \Delta R)^3\, 2\rho_1\,(1/2)\,e_c$, where e_c is the chemical energy per unit mass of liquid propellants and ρ_1 is the gas density ahead of the front. As in Section II, the medium ahead of the front is taken to be a 50%, by mass, mixture of burned gas and unburned liquid propellants. The *average* pressure within the r_0-sphere may be estimated as proportional to the thermal energy density in that region; therefore,

$$p_2 = A\left[\frac{\rho_1 e_1 \frac{4}{3}\pi r_0^3}{\frac{4}{3}\pi r_0^3} + \frac{\frac{4}{3}\pi\,(r_0 - \Delta R)^3\,\rho_1 e_c}{\frac{4}{3}\pi r_0^3} + \frac{E_{\text{blast}}}{\frac{4}{3}\pi r_0^3}\right] \tag{4}$$

[2]The detonation wave thickness is $(D^{C\text{-}J} - u_2)\tau$ where u_2 is the particle velocity behind the front; it will be seen that

$$\Delta R > D^{C\text{-}J}\tau > (D^{C\text{-}J} - u_2)\tau$$

for $u_2 > 0$.

In this equation, A is a proportionality constant; the first term in the brackets is the energy density due to gas swept up by the advancing front; the second term is the contribution from chemical heat release; the last term is the contribution from the initiating blast energy. The pressure ahead of the front is $p_1 = A\rho_1 e_1$. Then Eq. (4) becomes

$$\frac{p_2 - p_1}{A} = \left(1 - \frac{\Delta R}{r_0}\right)^3 \rho_1 e_c + \frac{E_{\text{blast}}}{\frac{4}{3}\pi r_0^3} \tag{5}$$

This equation exhibits the essential *average* features of the spherical wave. When $r_0 = \Delta R$, there is no effect of chemical reaction; when $r_0 >> \Delta R$, the blast energy contribution is negligible. For $r_0/\Delta R = \infty$,

$$\frac{p_{2,\infty} - p_1}{A} = \rho_1 e_c$$

Therefore, the proportionality constant A may be written as

$$A = \frac{p_{2,\infty} - p_1}{\rho_1 e_c}$$

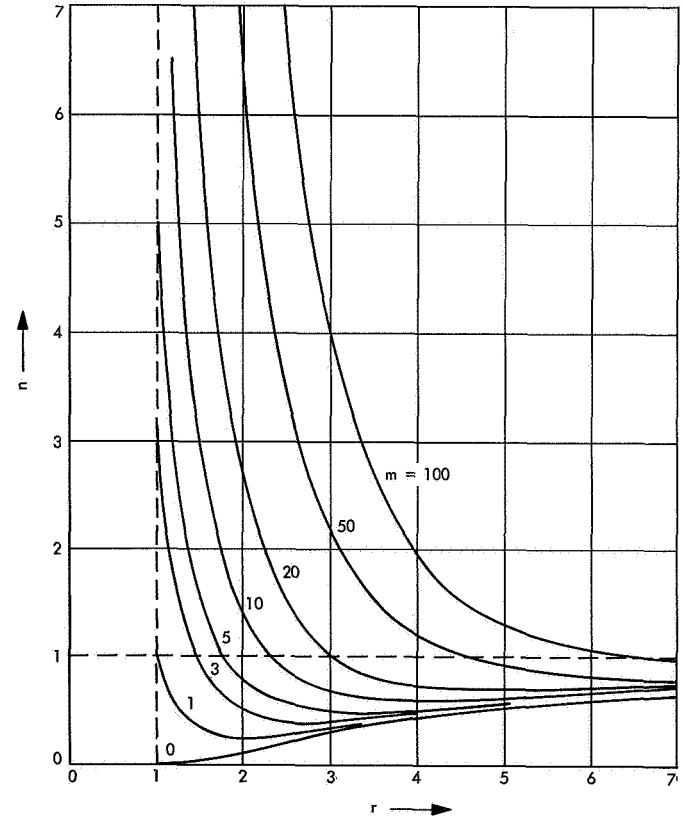

Fig. 3. Spherical detonation wave according to Eq. (6)

If nondimensional quantities are introduced, Eq. (5) becomes

$$n(r; m) = (1 - r^{-1})^3 + \frac{m}{r^3} \tag{6}$$

where

$$n = \frac{p_2 - p_1}{p_{2,\infty} - p_1}$$

$$m = \frac{U_2 E_{\text{blast}}}{(\Delta R)^3}, \qquad U_2 \equiv \frac{1}{\frac{4}{3}\pi\rho_1 e_c}$$

$$r = \frac{r_0}{\Delta R}$$

Equation (5) may be plotted in n, r space for various values of m (see Fig. 3). It is seen that n always approaches unity from a value less than 1.0 as $r \to \infty$; furthermore, n always has a minimum. The depth and location of that minimum depends upon the parameter m. From Eq. (6),

$$n(r_{\min}; m) \equiv n_{\min} = m/r_{\min}^2 \tag{7}$$

with

$$r_{\min} = 1 + m^{1/2} \tag{8}$$

From the definition of m and Eq. (3),

$$m = U_2 U_1^{-3} E_{\text{blast}}^{2/5} = \frac{E_{\text{blast}}^{2/5}}{\frac{4}{3}\pi\rho_1^{2/5} e_c \xi_0^3 \tau^{6/5}} \tag{9}$$

The physical implications of these results are as follows:

(1) Large m suggests that a spherical detonation *will* develop because $n_{\min}$ will be sufficiently large to ensure that the reaction region is always "close" to the shock front in the sense that the minimum pressure is not far below the final pressure $p_{2,\infty}$.

(2) The value of m depends upon the ratio $(E_{\text{blast}}/\tau^3)^{2/5}$ so that large E_{blast} and/or small chemical induction times contribute to the formation of spherical detonation waves.

(3) If τ is small, E_{blast} can be quite small.

Finally, it should be noted that m varies *inversely* as e_c. This may, at first, seem paradoxical, but small e_c (large m) implies small $(p_{2,\infty} - p_1)$ (a weak detonation wave). Therefore, $(p_2 - p_1)$ at $t = \tau$ (which is assumed independent of e_c) is much larger than $(p_{2,\infty} - p_1)$, and the weak detonation may be expected to develop. However, large e_c (small m) implies large $(p_{2,\infty} - p_1)$ (a strong detonation wave); in this case, $p_2 - p_1$ at $t = \tau$ can be much smaller than $(p_{2,\infty} - p_1)$, which indicates that the pressure at the end of the blast wave portion is much below the final detonation pressure. Therefore, the final development phase (in which chemical reaction becomes important) may never occur.

It should be emphasized that the pressure p_2 computed using Eq. (6) is an average pressure within the sphere r_0; it is *not* the pressure behind the advancing front. This model can only give qualitative indications of the formation of a spherical detonation wave by an initiating blast.

Some computations were performed using the data of the Appendix; the results are summarized in Table 1.

Table 1. Zel'dovich, Kogarko, Simonov model for spherical detonation[a]

τ, s	$E_{\text{blast}}/E_{\text{chamber}}$	ΔR, cm	m	$r_{\min}$	$n_{\min}$	r_0, cm at $n_{\min}$	$E_{\text{chemical}}/E_{\text{blast}}$ at $n_{\min}$	$D^{C-J}\tau$, cm
10^{-5}	10^{-2}	3.97	1.28	2.13	0.280	8.45	1.11	2.67
10^{-6}	10^{-2}	1.58	20.2	5.5	0.67	8.7	4.42	0.267
10^{-7}	10^{-2}	0.63	320	18.9	0.89	11.9	17.7	0.0267
10^{-5}	10^{-3}	2.50	0.515	1.715	0.17	4.29	0.71	2.67
10^{-6}	10^{-3}	0.99	8	3.83	0.55	3.83	2.82	0.267
10^{-7}	10^{-3}	0.40	125	12.2	0.84	4.88	11.10	0.0267
10^{-5}	10^{-4}	1.58	0.20	1.45	0.10	2.28	0.48	2.67
10^{-6}	10^{-4}	0.63	3.20	2.79	0.41	1.76	1.80	0.267
10^{-7}	10^{-4}	0.254	48.8	7.98	0.77	2.03	6.98	0.0267

[a] $E_{\text{chamber}} = 0.74 \times 10^{12}$ g cm^2/s^2.
$\rho_1 = 4.36 \times 10^{-4}$ g/cm^3, $T_1 = 3100°$K.
$e_c = 5.05 \times 10^{10}$ cm^2/s^2.
$\xi_0^5 = 0.58$; $D^{C-J} = 2.67 \times 10^5$ cm/s, $(M^{C-J} = 2.17)$.

The choice of τ is most critical and least known. However, White (Ref. 8) and Strehlow et al. (Ref. 9) have shown that when gaseous detonations are initiated by reflected shocks, the time (measured from the instant of reflection) for initiation of chemical reactions is of the order of 50×10^{-6} s, decreasing with increasing temperature. This writer believes that the turbulent, hot, liquid–gas medium within a rocket chamber should have induction times no greater than those measured by White and Strehlow. Thus τ was taken as $\tau = 10^{-5}$, 10^{-6}, and 10^{-7} s.

For these values of τ and certain assumed values for E_{blast}, the results (see Table 1) show that the initiation of a detonation wave even for $E_{blast} << E_{chamber}$ seems to be possible. The column marked "$E_{chemical}/E_{blast}$ at n_{min}" exhibits the ratio of liberated chemical energy behind the front to blast energy when the wave is at r_{min}; this ratio is substantially greater than unity except for $\tau = 10^{-5}$ s. This shows that accumulated chemical energy release is greater than the blast energy even as close to the point of initiation as the minimum pressure point.

The last column, denoted by $D^{C-J}\tau$, gives the induction distance based on the steady Chapman–Jouguet detonation velocity for a medium with $e_c = 1200$ cal/g and $T_1 = 3100°$K. In almost all cases this distance is less than ΔR; the use of $D^{C-J}\tau$ instead of ΔR would have given larger values of m (in those cases where $D^{C-J}\tau < \Delta R$) and therefore more favorable circumstances for the existence of detonations.

If τ can be as small as 10^{-7} s, then an $E_{blast}/E_{chamber}$ as small as 10^{-4} can result in an essentially fully developed detonation wave within 2.03 cm of the point of initiation. This implies that detonation-like waves can be expected in rocket chambers. Their importance depends upon their amplitude and their potential for coupling into some unsteady resonant mode of combustion in the chamber, especially the rotating mode.

It is generally recognized that high-amplitude resonance is initiated less frequently in rocket engines of lesser combustion efficiency and/or smaller chamber volume. This tendency is consistent with the Zel'dovich, Kogarko, Simonov model of spherical detonation initiation. If a spherical detonation is to develop, then m must be large enough that n_{min} is not too small; see Eq. (7). Furthermore, if $E_{blast}/E_{chamber}$ is designated as ϵ and if it is assumed that $\epsilon < 1.0$, then with $E_{chamber} = \alpha\rho_1 V_{chamber} e_c$, where α is a proportionality constant, $E_{blast} = \epsilon\alpha\rho_1 V_{chamber} e_c$ and, from Eq. (9),

$$m = \left[\frac{(\epsilon\alpha)^{2/5}}{\frac{4}{3}\pi\xi_0^3}\right] V_{chamber}^{2/5} (e_c \tau^2)^{-3/5}$$

This result shows, among other interrelationships, that (1) small $V_{chamber}$ and/or large $e_c\tau^2$ (lesser combustion efficiency) implies small m; i.e., operation less susceptible to the generation of detonative disturbances from local "blasts" and (2) small $e_c\tau^2$ (good combustion efficiency resulting in small effective e_c and small τ) implies large m; i.e., the opposite of the trend above. But small e_c also implies weak detonations, so that even though the detonation is likely to develop, its amplitude may be small.

This line of reasoning allows one to construct the following picture of nonlinear rocket engine stability without mechanical damping:

(1) Inefficient or small engines will exhibit a relatively large margin of stability to finite disturbances.

(2) If, however, detonative waves do develop, they will have large amplitudes.

(3) Efficient or large engines will tend to have a small margin of stability.

In such engines (i.e., those without mechanical damping), detonative waves are easily formed, and although they are smaller in amplitude (their amplitudes decreasing as the efficiency increases), they can be large enough to trigger resonant modes of combustion. A particularly unfavorable circumstance is that where the detonation initiation occurs in a region of relatively complete combustion (low effective e_c and small τ) and is able to propagate into a region of large effective e_c (near the injector, for instance).

The next section discusses the amplitude of Chapman–Jouguet detonations in the rocket chamber regime and the interaction of waves with walls and gaseous interfaces.

IV. The Interaction of Reactive Wave Fronts With Walls and Gaseous Interfaces

A. Phenomenological Description and Analytical Formulation

The presence of the rocket chamber walls causes any incident detonation or shock wave to be reflected. Thus

the gas behind the reflected front will have substantially different thermodynamic properties from that behind the incident front. This is of importance because pressure transducers most likely measure pressure in the reflected region (see Fig. 1, which depicts normal reflection).

It is also possible that the gas adjacent to a cool wall will be substantially cooler than that in the interior of the chamber. Then the incident wave front is propagating toward the wall through an inhomogeneous medium. If the inhomogeneity is idealized as a layer of cool gas adjacent to a layer of hot gas, the interface is some surface which the incident shock or detonation wave encounters on its passage toward the wall. It will be seen that this hot–cold interface can have a considerable effect on the properties of the gas adjacent to the wall after reflection.

All of the following analysis will assume planar wave fronts and parallel planar interfaces and walls. This will enable rather straightforward computations, but still yield meaningful results; the object is to elucidate the phenomena without becoming embedded in serious computational difficulties.

All discussions involving discontinuous changes in flow properties begin with the Rankine–Hugoniot relations. Their derivation may be found in many texts (Refs. 5, 6, 10, 11, and 12). A form of the Rankine–Hugoniot equations for detonations in dilute sprays was derived by Williams (Ref. 13); his results show that order-of-magnitude changes in detonation properties will not arise in the presence of finely dispersed liquid droplets. We shall, therefore, not employ his formulation in these computations. One form, which can be derived from the standard formulation and is valid for an ideal gas, that will be useful for us is the following:

$$\left(\frac{\delta_1}{c_1}\right)^2 - \frac{2}{\gamma_2+1} M_1\left(1 - \frac{\gamma_2}{\gamma_1} M_1^{-2}\right)\frac{\delta_1}{c_1} + \frac{Q_1^2}{(\gamma_2+1)^2} = 0 \tag{10}$$

$$\frac{p_2}{p_1} = 1 + \gamma_1 M_1 \frac{\delta_1}{c_1} \tag{11}$$

$$\frac{\rho_2}{\rho_1} = M_1\left(M_1 - \frac{\delta_1}{c_1}\right)^{-1} \tag{12}$$

where

$$\delta_1 = u_2 - u_1$$

$$M_1 = \frac{D_1 - u_1}{c_1}$$

$$c_1 = \left(\frac{\gamma_1 p_1}{\rho_1}\right)^{1/2}$$

$$Q_1^2 = 2(\gamma_2^2 - 1)\left[\frac{q_1 - q_2}{c_1^2} - \frac{\gamma_1 - \gamma_2}{\gamma_1(\gamma_1 - 1)(\gamma_2 - 1)}\right]$$

In these equations, u_1 and u_2 are the fluid velocities ahead of and behind the front; D_1 is the velocity of the front; c_1 is the sonic velocity in region 1; M_1 is the mach number of the front with respect to the gas ahead of the front; $q_1 - q_2$ is the effective thermal energy release per unit mass of medium (1) due to chemical reaction; γ_1 and γ_2 are the ratios of the specific heats ahead of and behind the front.

These equations are valid for $D_1 > u_1$, i.e., fluid (1) being transformed into fluid (2). The term γ_2 is not an independent parameter; it is determined from the thermodynamic state of the gas behind the front.

From Eq. (10), we obtain

$$\frac{\delta_1}{c_1} = \frac{M_1\left(1 - \frac{\gamma_2}{\gamma_1 M_1^2}\right)}{\gamma_2 + 1}\left\{1 \pm \left[1 - \frac{Q_1^2}{M_1^2\left(1 - \frac{\gamma_2}{\gamma_1 M_1^2}\right)^2}\right]^{1/2}\right\} \tag{13}$$

where, with M_1, γ_2, γ_1, and Q_1 prescribed, the relative velocity δ_1 is determined. The plus sign corresponds to an overdriven wave; the minus sign to an underdriven wave.

If $M_1 > (\gamma_2/\gamma_1)^{1/2}$, then $\delta_1 > 0$; this is a detonation.

If $M_1 < (\gamma_2/\gamma_1)^{1/2}$, then $\delta_1 < 0$; this is a deflagration.

The critical value for M_1 occurs when the quantity shown to the ½ power in Eq. (13) is zero. Then

$$M_1\left(1 - \frac{\gamma_2}{\gamma_1} M_1^{-2}\right) = \pm Q_1$$

The two positive values of M_1 that satisfy this equation are the Chapman–Jouguet values for detonation and

deflagration. They are

$$M_1 \equiv M_1^{C\text{-}J} = \frac{1}{2}\left[\pm Q_1 - \left(Q_1 + 4\frac{\gamma_2}{\gamma_1}\right)^{1/2}\right] \tag{14}$$

For these values of M_1,

$$\left(\frac{\delta_1}{c_1}\right)^{C\text{-}J} = \frac{\pm Q_1}{\gamma_2 + 1} \tag{15}$$

and the corresponding Chapman–Jouguet pressure and density ratios follow from Eqs. (11) and (12).

In this section, several computations will be performed assuming that the incident front is a Chapman–Jouguet detonation.

B. Reflection of Chapman–Jouguet Detonation as a Shock Wave

Figure 4 is a schematic diagram of the wave front phenomenon. If the incident front is a Chapman–Jouguet detonation, then all flow properties in region (2) are known via Eqs. (14) and (15). The reflected shock front must be strong enough to cause $u_3 = 0$. We assume $\gamma_1 = \gamma_2 = \gamma_3$.

For

$$q_1 - q_2 = \frac{1}{2} \times 1200\ \text{cal/g} = 2.52 \times 10^6\ \text{m}^2/\text{s}^2$$

one finds that

$$c_1^2 = 1.51 \times 10^6\ \text{m}^2/\text{s}^2$$

based on

$T_1 = 3100°\text{K}$

$\gamma_1 = 1.2$

Molecular weight $\cong 20$

$Q_1^2 = 1.47$

$M_1^{C\text{-}J} = 1.77$

$(\delta_1/c_1)^{C\text{-}J} = 0.551$

$(p_2/p_1)^{C\text{-}J} = 2.172$

$(\rho_2/\rho_1)^{C\text{-}J} = 1.45$

Note that the Chapman–Jouguet detonation for this case is not particularly strong. This is due to the high temperature of the rocket chamber medium. The parameter of importance is $(q_1 - q_2)/c_1^2$, not $q_1 - q_2$ alone.

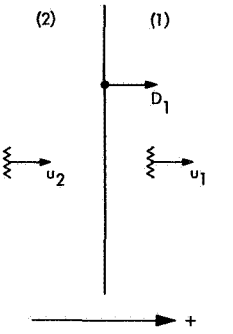

Fig. 4. Motion of wave front; u_1 and u_2 are particle velocities; D_1 is the wave front velocity. The signed arrow indicates positive values of velocities

Across the reflected front, Eqs. (10–12) become

$$\left(\frac{\delta_2}{c_2}\right)^2 - \frac{2}{\gamma_3 + 1} M_2\left(1 - \frac{\gamma_3}{\gamma_2} M_2^{-2}\right)\frac{\delta_2}{c_2} + \frac{Q_2^2}{(\gamma_3 + 1)^2} = 0 \tag{16}$$

$$\frac{p_3}{p_2} = 1 + \gamma_2 M_2 \frac{\delta_2}{c_2} \tag{17}$$

$$\frac{\rho_3}{\rho_2} = \frac{M_2}{M_2 - \dfrac{\delta_2}{c_2}} \tag{18}$$

where

$$\delta_2 = u_3 - u_2$$

$$M_2 = \frac{-D_2 - u_2}{c_2}$$

$$c_2^2 = c_1^2 \frac{p_2/p_1}{\rho_2/\rho_1}$$

If $Q_2 = 0$ and if $\gamma_3 = \gamma_2 = \gamma_1$, then

$$M_2(1 - M_2^{-2}) = \frac{\gamma_1 + 1}{2}\frac{\delta_2}{c_2} \tag{19}$$

But

$$\delta_2 = -u_2 = -\delta_1 \text{ if } u_3 = u_1 = 0$$

and then

$$\delta_2/c_2 = -\left(\frac{\delta_1}{c_1}\right)\left(\frac{c_1}{c_2}\right)$$

For the known properties of the incident Chapman–Jouguet wave,

$$\frac{\delta_2}{c_2} = -0.45$$

Then Eq. (19) yields

$$M_2 = -1.28$$

From Eq. (17),

$$\frac{p_3}{p_2} = 1.692$$

The overall reflected pressure ratio is then

$$\frac{p_3}{p_1} = \frac{p_3}{p_2}\frac{p_2}{p_1} = 3.67$$

We conclude that

(1) A Chapman–Jouguet detonation in the rocket chamber medium ($Q_1^2 = 1.47$) results in a rather small pressure rise, $(p_2/p_1)^{C-J} = 2.172$.

(2) Upon normal reflection as a shock wave, the overall pressure ratio becomes $p_3/p_1 = 3.67$.

Clayton observes pressure ratios at the wall of ~7. It should be noted that if $q_1 - q_2 = 1200$ cal/g so that $Q_1^2 = 2.93$, then

$$M_1^{C-J} = 2.17 \qquad M_2 = -1.35$$

$$\left(\frac{\delta_1}{c_1}\right)^{C-J} = 0.778 \qquad \frac{\delta_2}{c_2} = -0.556$$

$$\left(\frac{p_2}{p_1}\right)^{C-J} = 3.02 \qquad \frac{p_3}{p_2} = 1.91$$

$$\left(\frac{\rho_2}{\rho_1}\right)^{C-J} = 1.56 \qquad \frac{p_3}{p_1} = 5.75$$

Even the full available chemical energy does not yield pressure ratios as high as 7.

C. Reflection of Chapman–Jouguet Detonation in the Presence of a Gaseous Interface

Since the chamber wall is cold compared with the combustion gases, any incident wave will pass through a layer of relatively cool gas before encountering the wall. This process will be seen to have an amplification effect on the overall reflected pressure ratio; i.e., the pressure at the wall increases because of the presence of the cool gas layer.

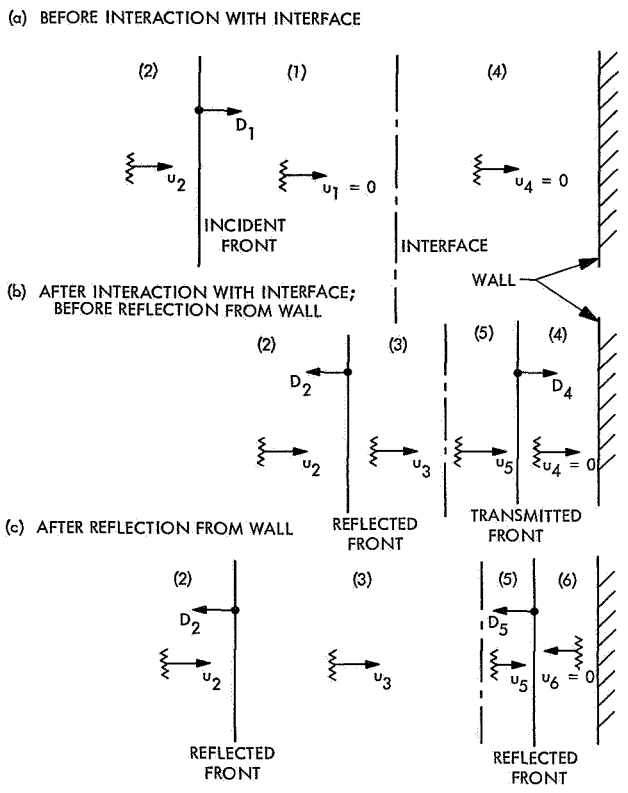

Fig. 5. Transmission and reflection of wave front at gaseous interface; reflection of transmitted wave from wall

The sequence of events is shown schematically in Fig. 5. Computation of the several states of the gases and the motion of the shocks and interface proceeds as follows (all values of γ are assumed to be equal to 1.2):

If the D_1-wave is assumed to be a Chapman–Jouguet detonation, then one can write

$$M_1 = M_1^{C-J} = \frac{1}{2}\left[Q_1 + (Q_1^2 + 4)^{1/2}\right]$$

$$\left(\frac{\delta_1}{c_1}\right)^{C-J} = \frac{Q_1}{\gamma + 1}$$

$$\left(\frac{p_2}{p_1}\right)^{C-J} = 1 + \gamma M_1^{C-J}\left(\frac{\delta_1}{c_1}\right)^{C-J}$$

$$\left(\frac{\rho_2}{\rho_1}\right)^{C-J} = \frac{M_1^{C-J}}{M_1^{C-J} - (\delta_1/c_1)^{C-J}}$$

$$\frac{c_1}{c_2} = \left[\left(\frac{\rho_2}{\rho_1}\right)^{C-J}\right]^{1/2}\left[\left(\frac{p_2}{p_1}\right)^{C-J}\right]^{-1/2}$$

And when $u_1 = 0$ and $Q_2 = 0$, one can write, for the D_2-wave,

$$\frac{\delta_2}{c_2} = \frac{c_1}{c_2}\left(\frac{u_3}{c_1} - \frac{\delta_1}{c_1}\right)$$

$$M_2(1 - M_2^{-2}) = \left(\frac{\gamma + 1}{2}\right)\frac{\delta_2}{c_2}$$

$$\frac{p_3}{p_2} = 1 + \gamma M_2 \frac{\delta_2}{c_2}$$

Thus for a prescribed u_3/c_1, the D_2-wave is determined.

The conditions at the interface are given by

$$p_4 = p_1, \qquad p_3 = p_5, \qquad u_3 = u_5$$

And for $u_4 = 0$, the pressure ratio across the D_4-wave is

$$\frac{p_5}{p_4} = \frac{p_3}{p_1} = \frac{p_3}{p_2}\frac{p_2}{p_1} \tag{20}$$

Thus p_5/p_4 is determined when u_3/c_1 is prescribed. Furthermore,

$$\frac{\delta_4}{c_4} = \frac{u_5 - u_4}{c_4} = \frac{u_5}{c_4}$$

$$= \frac{u_3}{c_1}\frac{c_1}{c_4}$$

Since $c_1/c_4 = (T_1/T_4)^{1/2}$ is a given quantity, δ_4/c_4 is determined once u_3/c_1 is prescribed:

$$M_4(1 - M_4^{-2}) = \frac{\gamma + 1}{2}\left(\frac{\delta_4}{c_4}\right)\left[1 + \frac{\dfrac{Q_4^2}{(\gamma + 1)^2}}{\left(\dfrac{\delta_4}{c_4}\right)^2}\right]$$

$$\frac{p_5}{p_4} = 1 + \gamma M_4 \frac{\delta_4}{c_4} \tag{21}$$

We see that both Eqs. (20) and (21) yield p_5/p_4. Therefore, u_3/c_1 must be chosen such that values of p_5/p_4 as computed from Eqs. (20) and (21) are equal.

For $u_6 = 0$ and $Q_5 = 0$, the D_5-wave properties are given by

$$\frac{\delta_5}{c_5} = -\frac{\delta_4}{c_4}\frac{c_4}{c_5}$$

$$\frac{c_4}{c_5} = \left[\left(\frac{p_4}{p_5}\right)\left(\frac{\rho_5}{\rho_4}\right)\right]^{1/2}$$

$$M_5(1 - M_5^{-2}) = \frac{\gamma + 1}{2}\frac{\delta_5}{c_5}$$

$$\frac{p_6}{p_5} = 1 + \gamma M_5 \frac{\delta_5}{c_5}$$

Finally, the overall pressure ratio is given by

$$\frac{p_6}{p_4} = \frac{p_6}{p_1} = \frac{p_6}{p_5}\frac{p_5}{p_4} \tag{22}$$

Some numerical results are shown in Fig. 6 for the case of a Chapman–Jouguet detonation as the incident wave. The lower curve corresponds to the assumption that chemical heat release in the cool gas, region (4), remains equal to that in the hot gas, region (1). The upper curve corresponds to the assumption that chemical heat release is negligible in the cool gas.

When heat release persists in the cool gas, the overall pressure ratio is less than it would be if there were no heat release in the cool gas, this being true for all the computed values of $c_1/c_4 = (T_1/T_4)^{1/2}$.

With $Q_4 \neq 0$ and $u_3/c_1 \to 0$, we see that $M_4 \to \infty$ while p_5/p_4 remains finite. However, if $Q_4 = 0$, then δ_4/c_4 cannot approach zero since this would yield $M_4 \to 1$ and $p_5/p_4 \to 1$ from Eq. (21), while Eq. (20) gives $p_5/p_4 \neq 1$. Therefore, $\delta_4/c_4 = (u_3/c_1)(c_1/c_4)$ must remain finite as $u_3/c_1 \to 0$ and thus c_1/c_4 must get large in this limit. In other words, if $Q_4 = 0$, then larger c_1/c_4 corresponds to

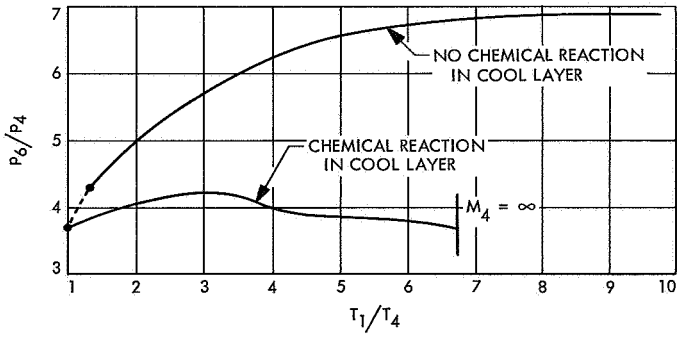

Fig. 6. Overall reflected pressure ratio as function of temperature ratio at gaseous interface

smaller u_3/c_1. This requires a stronger D_2-wave with higher pressure ratio p_3/p_2; it results ultimately in a *larger* overall pressure ratio p_6/p_4.

The presence of the "hot–cold" gaseous interface in the neighborhood of the wall does increase the overall pressure ratio, the increase being greatest when chemical reaction in the cool layer is quenched.

It may be reasonable to assume that $T_1/T_4 \cong 8$; then $p_6/p_4 = 6.8$, which is quite close to Clayton's observed value.

Finally, it should be added that the quenching of the chemical reaction in the cool layer is very likely; not only will the lower temperature contribute to this possibility, but as $u_3/c_1 \to 0$, $D_4 \to \infty$ so that chemical reaction behind the D_4-wave could not keep up with the wave front.

V. The Transition of Spherical Detonation to a Rotating Combustion Disturbance

In Section III, the initiation of a spherical detonation wave was shown to be possible within the constraints of the assumed rocket engine data. The interaction of the detonation with walls and gaseous interfaces, as discussed in Section IV, results in pressure ratios close to those observed by Clayton. It remains to explain how the initially spherical detonation becomes the circumferentially rotating combustion disturbance observed during the fully developed resonant burning mode.

The arguments to be presented are only descriptive in nature; they give a plausible explanation for the evolution of the rotating detonative disturbance. Quantitative data or computations are still to be developed.

In Fig. 7 is shown a sequence of events that can lead to a rotating disturbance from an off-axis disturbance:

(1) The spherical detonation front reaches the wall at point A in Fig. 7a and begins to reflect; because of inhomogeneities in the hot, liquid–gas medium within the chamber, the reflected front moves faster in the right-hand portion, say, than in the left-hand portion of the chamber.

(2) As the reflecting wave converges toward point B in Fig. 7a, the fluid medium in its wake is induced to flow from right to left because the detonative front sweeping across the right-hand portion of the chamber has a higher pressure in its wake than that sweeping across the left-hand portion; this produces

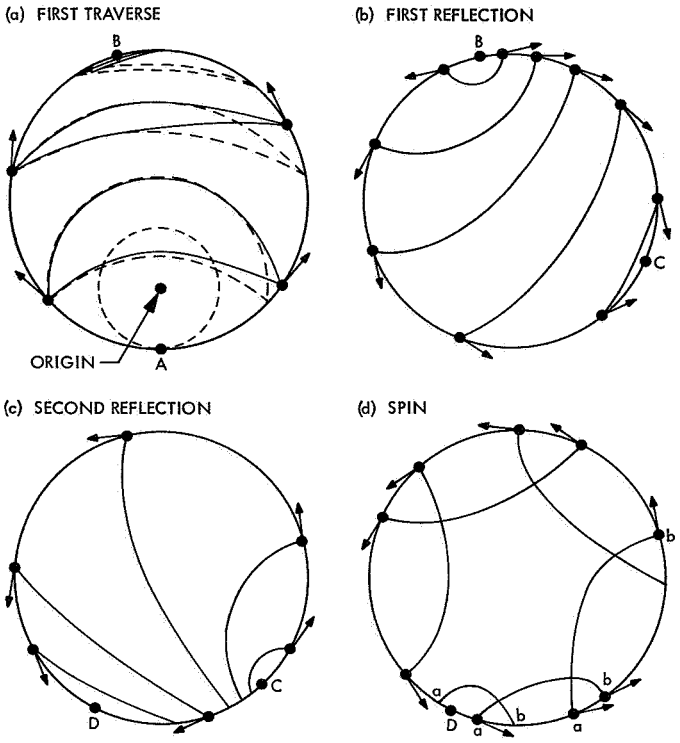

Fig. 7. Transition of a spherical detonation to a rotating combustion disturbance

an enhancement of the available chemical energy on the left as compared with the right (at least near the injector face) because the reactants are deflected by the right–left gas flow.

(3) The reflecting wave emerging from point B, Fig. 7b, now faces a medium with larger available chemical energy on the left than on the right; the reflecting detonative front converging toward point C moves with greater strength along the left side of the chamber; and a fluid flow is induced from left to right, causing the same effect as described in step (2).

(4) If the sloshing fluid flow results in an amplification of the initial chemical inhomogeneity, the wave emanating from point C will converge, say, at point D (Fig. 7c).

(5) Let us assume that by this time the chemical inhomogeneity is such that the reflected wave from point D (Fig. 7d) sees a medium that has virtually no available chemical energy on its left; then it will move in an essentially one-sided fashion, counterclockwise in this example, around the chamber. This configuration continues to move in a peripheral manner and is the resonant mode observed.

Clayton[3] has taken high-speed motion pictures showing the initiation of the rotating mode of combustion; one can observe the general features described above, including the "sloshing" behavior of the gas motion. Burstein (Refs. 14 and 15) has performed numerical experiments with a rotating wave in a noncombustible gas with cylindrical symmetry; he also gets a gas motion which has a strong radial component that is nonzero at the origin ("sloshing").

VI. Conclusions

It has been shown that a blast wave, of itself, in general cannot account for the large-amplitude pressure pulse that seems to initiate resonant burning in rocket engine chambers. A blast wave of such magnitude would require energy of the order of that available in the chamber.

Using a theory for the initiation of spherical detonation, due to Zel'dovich, Kogarko, and Simonov, computations were performed which indicate that it is possible to initiate detonations in the rocket chamber using a small percentage of the available chemical energy if the chemical induction time is small enough. The literature on chemical induction times in conjunction with shock waves indicates that a time of 10^{-6} s or less is reasonable; with such times, the fraction of chemical energy in the chamber for detonation initiation may be as small as 10^{-3}.

[3]See Footnote 1.

The detonation waves in the chamber, if they are of the Chapman–Jouguet type, do not possess large pressure ratios. This is the consequence of the state conditions existing in a typical rocket engine. (See, for example, the illustration utilizing typically high temperatures and pressure, in Section IV-B.) The controlling variable is chemical heat release per unit mass divided by the local sonic velocity squared. However, if account is taken of the low-temperature gas layer adjacent to the rocket walls, a significant amplification of the reflected pressure ratio is present; in these circumstances the reflected pressure ratio at the wall becomes approximately that observed.

A description of the transition from a spherical detonation to a circumferential disturbance is presented, which may account for the observed rotational character of the resonant mode of burning. Its verification will depend upon extensive measurements of flow properties within the chamber during the transition period.

This analysis suggests that large-amplitude, high-frequency resonant burning is a very probable event. Its presence is enhanced by high temperatures, nearly complete combustion, and the relative ease with which a spherical disturbance may transform to a rotating disturbance. Complete combustion and baffles that can inhibit the rotating mode may be factors in minimizing or preventing its occurrence.

Nomenclature

A proportionality constant

c sonic velocity, cm/s

D wave front velocity, cm/s

E_{blast} blast wave energy and initiation energy for spherical detonation, $\text{kg m}^2/\text{s}^2$

E_{chamber} available chemical energy in chamber, $\text{kg m}^2/\text{s}^2$

E_{chemical} chemical energy liberated behind wave front, $\text{kg m}^2/\text{s}^2$

e_c chemical energy per unit mass of propellants, m^2/s^2

e_1 thermal energy per unit mass of medium ahead of incident front, m^2/s^2

M Mach number

$\overline{M}$ molecular weight

M_g mass of gas, kg_m

M_l mass of liquid, kg_m

m nondimensional parameter in Eq. (6)

n nondimensional parameter in Eq. (6)

p pressure, dyn/cm^2

q available chemical energy, m^2/s^2

Nomenclature (contd)

Q nondimensional heat release parameter in Eq. (10)

R gas constant, specific, $= R_0/\overline{M}$

R_0 gas constant, universal

ΔR thickness of reaction zone, cm

r nondimensional parameter in Eq. (6)

r_0 radius of blast wave or detonation wave, cm

T temperature, °K

u fluid particle velocity, cm/s

V_{chamber} chamber volume

δ velocity difference across wave front, cm/s

ϵ $E_{\text{blast}}/E_{\text{chamber}}$

γ ratio of specific heats

ξ_0 a mathematical constant in blast wave theory

τ chemical induction time, s

U_1 defined as $\xi_0 \tau^{2/5}/\rho_1^{1/5}$

U_2 defined as $1/[(4/3)\pi\rho_2 e_c]$

Subscripts

(Numbers refer to Fig. 5)

1 ahead of incident wave front

2 behind incident wave front

3 behind reflected wave front

4 ahead of transmitted wave front

5 behind transmitted wave front

6 behind reflected wave front

min minimum value

Superscripts

C-J Chapman–Jouguet detonation

References

1. Weiss, R. R., *An Introduction to Combustion Instability in Liquid Propellant Rocket Engines*, RPL TR-66-150. Rocket Propulsion Laboratory, U.S. Air Force Systems Command, Research and Technology Division, July 1966.
2. Clayton, R. M., Rogero, R. S., and Sotter, J. G., "An Experimental Description of Destructive Liquid Rocket Resonant Combustion," *AIAA J.*, Vol. 6, No. 7, pp. 1252–1259, July 1968.
3. Crocco, L., and Cheng, Sin-I, *Theory of Combustion Instability in Liquid Propellant Rocket Motors*, Butterworth & Co., Ltd., London, 1956.
4. Bonnell, J. M., *An Investigation of Spherical Blast Waves and Detonation Waves in a Rocket Combustion Chamber*, TR 32-1286. Jet Propulsion Laboratory, Pasadena, Calif., Aug. 15, 1968.
5. Landau, L. D., and Lifshitz, E. M., *Fluid Mechanics*, p. 393. Pergamon Press, London, 1959.
6. Courant, R., and Friedrichs, K. O., *Supersonic Flow and Shock Waves*, p. 154. Interscience Publishers, Inc., New York, 1948.

References (contd)

7. Zel'dovich, Ia. B., Kogarko, S. M., and Simonov, N. N., "An Experimental Investigation of Spherical Detonation in Gases," *Soviet Phys.–JETP*, Vol. 1, p. 1689, 1957.

8. White, D. R., *A Study of Shock Wave Induced Reactions*, ARL-66-0177. Aerospace Research Laboratories, U.S. Air Force, Sept. 1966.

9. Gilbert, R. B., and Strehlow, R. A., "Theory of Detonation Initiation Behind Reflected Shock Waves," *AIAA J.*, Vol. 4, p. 1777, Oct. 1966.

10. Shchelkin, K. I., and Troshin, Ya. K., *Gasdynamics of Combustion*, Mono Book Corp., Baltimore, 1965.

11. Sokolik, A. S., *Self-Ignition, Flame and Detonation in Gases*, TT-63-11179, NASA Technical Translation F-125. (Translation of a monograph, *Samovosplamenenie, Plamya i Detonatsiya v Gazahk*, Moscow, 1960.) Translated by N. Kaner, 1963. Available from the Office of Technical Services, Department of Commerce, Washington, D.C.

12. Soloukin, R. I., *Shock Waves and Detonations in Gases*, Mono Book Corp., Baltimore, 1966.

13. Williams, F. A., "Detonations in Dilute Sprays," in *Detonation and Two-Phase Flow*, Vol. 6 of *Progress in Astronautics and Rocketry*, pp. 99–114. Edited by S. S. Penner and F. A. Williams, Academic Press Inc., New York, 1962.

14. Burstein, S. Z., and Chinitz, W., "Non-linear Combustion Instability in Liquid-Propellant Rocket Motors," Second Quarterly Report. Mathematical Applications Group, Inc., White Plains, N.Y., Jan. 30, 1968.

15. Burstein, S. Z., and Chinitz, W., "Non-linear Combustion Instability in Liquid-Propellant Rocket Motors," Third Quarterly Report. Mathematical Applications Group, Inc., White Plains, N.Y., April 30, 1968.

Appendix
Rocket Motor and Thermochemical Data

Test data were as follows:

(1) Propellants were N_2O_4 and a 50% (by weight) mixture of $N_2H_4 + N_2H_8C_2$.

(2) Propellant flow rate = 70 lbm/s.

(3) Chamber pressure = 80 psia.

(4) Heat release = 1200 cal/g of propellant mixture at an oxidizer–fuel ratio of 2.00.

(5) Adiabatic flame temperature = 3100°K.

(6) Thrust = 15,000 lbf.

(7) Equilibrium composition of products per mole:

0.33 N_2 0.36 H_2O 0.10 H_2 0.09 CO 0.04 CO_2 0.03 H 0.05 miscellaneous	average molecular weight $\cong$ 20.4

(8) Chamber dimensions = 18 in. diameter; 15.9 in. length.

(9) Ratio of specific heats $\gamma \cong 1.2$.